ESTERIFICATION OF FREE FATTY ACID FROM SLUDGE PALM OIL USING ZEOLITE-SULFONATED CARBON FROM SUGAR CANE CATALYSTS

HASANUDIN[1,2]*; WAN RYAN ASRI[1,2]; TRI ELTIYAH MUTHIARANI[1,2]; DAVID BAHRAIN[3] and FITRI HADIAH[3]

ABSTRACT

In this research, the zeolite-sulfonated carbon from sugar cane catalyst has been employed for the free fatty acid (FFA) esterification in sludge palm oil (SPO) optimised by response surface methodology and central composite design. The effect of the catalyst weight ratio of zeolite to sulfonated carbon was evaluated. The result showed that the catalyst with a weight ratio of zeolite to sulfonated carbon of 1:3 (% w/w) had the highest acidic value of 10.80 mmol g^{-1} and was used for further esterification optimisation. FTIR and EDX analysis affirmed the existence of a sulfonated group of the composite catalysts. The ^{13}C NMR analysis showed that the esterification successfully produced an ester compound. The optimum conditions for FFA conversion were acquired at a reaction temperature of 78.98°C, a reaction time of 119.97 min, a catalyst weight of 2.97 g, with 94.19% FFA conversion, and followed by a statistically significant model. The catalyst reusability study revealed that the catalyst had a slight decrease in catalyst performance and could generate up to 80.00% conversion after the fourth cycle. This study could bring forth early information about the potential of zeolite-sulfonated carbon from sugar cane catalyst for FFA conversion from SPO into high-value ester products.

INTRODUCTION

Crude palm oil (CPO) is an essential resource in Indonesia and has grown as one of the world's biggest producers, with Indonesia accounting for more than half of global CPO production. In recent decades, CPO production in Indonesia has surged from 0.84 million tonnes in 2001 to about 27.00 million tonnes in 2017 (Nasution *et al.*, 2018a; Rahman *et al.*, 2021). CPO production tends to increase every year by 1.50%-10.96%, resulting in a significant accumulation of by-products. Besides empty fruit bunches (EFB), shells, and fibres as palm oil by-products (Nasution *et al.*, 2018b), liquid waste palm oil mill effluent (POME) is reported as the most considerable waste fraction of the palm oil sector, wherein sludge palm oil (SPO) is the major oil residue observed in the top layer of POME (Tang *et al.*, 2020). Extraction of free fatty acids (FFA) from SPO has been carried out to increase the value of waste (Goh *et al.*, 2019). SPO is also reported to have been used as a feedstock for the production of biogas (Garritano *et al.*, 2018). On the other hand, it has a relatively high content of FFA (>20%) and is low-cost (USD1 t^{-1}); hence it has the potential to be utilised as biodiesel feedstocks (Abdullah *et al.*, 2017; Liu *et al.*, 2021; Muanruksa and Kaewkannetra, 2020).

1   Department of Chemistry,
    Faculty of Mathematics and Natural Science,
    Universitas Sriwijaya, Indralaya,
    30662 South Sumatra, Indonesia.

2   Biofuel Research Group,
    Faculty of Mathematics and Natural Science,
    Universitas Sriwijaya, Indralaya,
    30662 South Sumatra, Indonesia.

3   Department of Chemical Engineering,
    Faculty of Engineering,
    Universitas Sriwijaya, Indralaya,
    30662 South Sumatra, Indonesia.

*   Corresponding author e-mail: hasanudin@mipa.unsri.ac.id

Biodiesel can be generated through transesterification using a homogeneous alkaline catalyst such as KOH (Abdullah *et al.*, 2017) and NaOH (Aslan and Eryilmaz, 2020). However, the high FFA content in SPO makes homogeneous alkaline catalysts to produce soap, prompting a drastic decline in conversion and biodiesel yield and complicating the separation process (dos Santos *et al.*, 2019). Esterification pretreatment can reduce the FFA content in SPO using homogeneous acid catalysts. Nevertheless, the catalyst is corrosive, produces water that reduces biodiesel products, and requires high biodiesel purifying costs (Anguebes-Franseschi *et al.*, 2018; Quah *et al.*, 2019). Heterogeneous acid catalysts based on oxides such as niobium oxide, heteropoly acids, resins, and carbon can substitute homogeneous acid catalysts. These catalysts are more economical in product separation and have good recyclability, but they require a longer reaction time, high catalyst loading, and low activity (Arumugamurthy *et al.*, 2019; Junior *et al.*, 2020). Heterogeneous carbon-based acid catalysts have fascinated much recognition due to the characteristics of a significant raw material source, have large surface functional groups, and exhibit high esterification catalytic activity (Zhang *et al.*, 2021).

One of the sources of a carbon-based catalyst that could behave as a catalyst in the esterification reaction is sugar cane. Studies show that the carbonisation of sugar cane produces amorphous carbon that can be easily functionalised (Balan *et al.*, 2021). Carbonised sugar cane is then sulfonated to increase stability and higher compactness of active sites (Tang *et al.*, 2018). Amorphous carbon with sulfonate groups ($-SO_3H$) on the surface provides excellent acidity (Fonseca *et al.*, 2020). Many studies report that sulfonated carbon catalysts from various feedstocks provide outstanding catalytic activity and properties (Farabi *et al.*, 2019; Ibrahim *et al.*, 2020; Ngaosuwan *et al.*, 2016; Tao *et al.*, 2015) sulfonated carbon-based catalysts are promising, economical, environment friendly, and can potentially replace sulfuric acid catalysts for industrial-scale esterification.

Supporting material with a large specific surface area and adequate catalytic activity is required to increase the ability of a sulfonated carbon catalyst, which could have a synergic effect in esterification. Zeolites are crystalline, porous, have Lewis and Brønsted acid sites, suitable as supporting materials (Ketzer *et al.*, 2020; Lawan *et al.*, 2020; Sun *et al.*, 2015). According to the literature review, composite zeolite-sulfonated carbon from sugar cane catalyst has not been reported yet for esterification of FFA from SPO. This catalyst was chosen for the study because the combination of sulfonated carbon with zeolite, where both materials have a high active catalytic site and good physicochemical properties,

could exhibit the synergic effect and promote high FFA conversion into esters. Therefore, this study would be focused on optimising FFA conversion derived from SPO utilising a zeolite-sulfonated carbon composite from a sugar cane catalyst using RSM-CCD. The advantages of the RSM-CCD result are high precision, good optimisation and can minimise experimental trials (Guo *et al.*, 2020; Kenawy *et al.*, 2019). The effect of the weight ratio of zeolite to sugar cane was also evaluated and the catalyst was characterised using FTIR, SEM-EDX, as well as acidity using the titration method. The input variables observed were the catalyst weight, reaction time and temperature, and the output variable observed was the FFA conversion into esters. The SPO and esterification products were analysed using ^{13}C-NMR.

MATERIALS AND METHODS

Materials

The materials utilised in this study were SPO waste (PT. Agro Indralaya Mandiri, Ogan Ilir, South Sumatra, Indonesia) and the fatty acid composition of SPO was assessed using gas chromatography (GC) (Shimadzu; using an HP-5 capillary column equipped with a flame ionisation detector and a flow rate of 3 mL min^{-1}), natural zeolite (Lampung), distilled water, sodium hydroxide, oxalic acid, phenolphthalein, methanol, sulfuric acid, hydrochloric acid, glacial acetate acid and anhydrous calcium dichloride. All chemicals were of analytical grade from Merck, New Jersey, USA.

Effect of Ratio of Zeolite to Sugar Cane

Natural zeolite was sieved with a 200-mesh, cleaned with distilled water, and then dried at 120°C in the oven for one day. Zeolite-sugar cane composites with a weight ratio of zeolite to sugar cane of 1:3, 1:2, 1:1, 2:1 and 3:1 (% w/w) were set out, and the solution subsequently was stirred using a magnetic stirrer at 300 rpm, temperature of 80°C for 1 hr. Zeolite-sugar cane composites were carbonised at 400°C using a furnace for 15 hr to produce zeolite-carbon composite.

Sulfonation of Zeolite-carbon Composite

A total of 20 g of the zeolite-carbon composite was mixed with 0.1 L of concentrated H_2SO_4. The solution was refluxed at 175°C for 15 hr and then washed with distilled water to neutral pH. The catalyst was dried at 120°C for one day. This result was then called a zeolite-sulfonated carbon composite.

Sludge Palm Oil (SPO) Esterification

The esterification was conducted using a batch reactor. Prior to esterification, the SPO was liquified in the oven at 80°C (Hayyan *et al.*, 2011). Afterwards, 25 g of liquified SPO was added with 75 mL methanol, followed by the zeolite-sulfonated carbon from sugar cane composite. The material was separated by centrifugation. The product was separated by adding distilled water (temperature around 70°C) to the separating funnel with 1:1 (v/v) between the esters and distilled water. The catalyst regeneration was conducted for reusability study by washing with ethanol and subsequently dried in the oven at 100°C. The determination of conversion of the reaction product was determined based on Equation (1) as follows:

$$\text{Conversion} (\%) = \frac{\text{Initial FFA - Final FFA}}{\text{Initial FFA}} \times 100 \quad (1)$$

SPO and products were then analysed using ^{13}C-NMR Bruker 300 MHZ with CDCl$_3$ solvent. The FFA content of SPO and products were determined using the titration method according to SNI 01-2901-2006 with the FFA content as palmitic acid.

Characterisation of Catalyst

The catalyst acidity strength was analysed using the titration method. Zeolite-sulfonated carbon composite, 1 g, was shacked with 0.1 L of 0.5 N NaOH for 24 hr. Afterwards, 5 mL of the mixture was taken and titrated with 0.1 N HCl. The amount of acid was defined as a difference between initial and final moles of NaOH divided by the catalyst weight. The functional groups of the as-synthesised catalyst were characterised using FTIR (Shimadzu), and the morphology surface of the catalyst was characterised using SEM-EDX (JEOL JSM-6300 Shimadzu).

Experimental Design using RSM-CCD

RSM is an experimental design-based technique for establishing the relationship between input and output variables. RSM can be used to model, analyse and optimise a process (Manojkumar *et al.*, 2020). The experimental design in this study used three input variables, X_1, X_2 and X_3, which were temperature (°C), catalyst weight (g), as well as reaction time (min), respectively, with the output variable being FFA conversion (Y). For the three variables in the experiment, the total number of experiments for three input variables was 17, including eight factorial and six axial points, as well as three replicates at the centre point. The variables were coded ± 1 referred to the factorial points, 0 for middle points, and ± α (± 1.68) for axial points. The ranges of the studied variables are shown in *Table 1*. Analysis of variance (ANOVA) was assessed to evaluate statistical parameters at the 95% confidence interval. Design Expert 12 software was used for the determination coefficient analysis of the model, plotting 3D response surfaces, as well as contour plots, whereas the coefficient R^2 determined the model's accuracy.
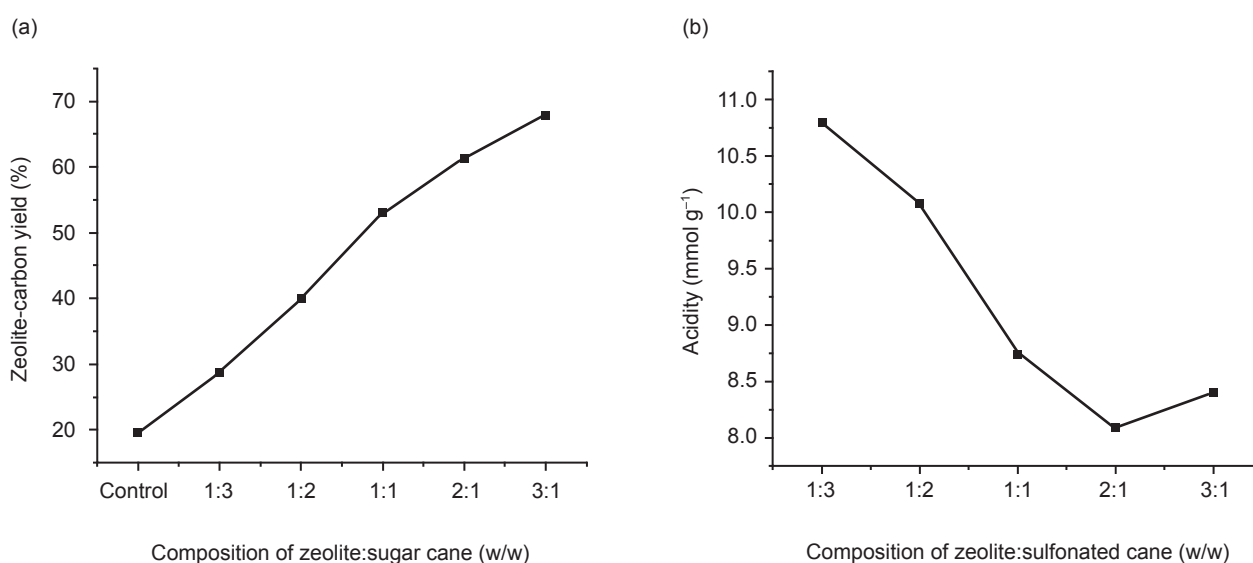

Figure 1. (a) The influence of zeolite weight ratio to sugarcane on zeolite-carbon yield, and (b) the influence of zeolite weight ratio to sulfonated carbon over catalyst acidity.

TABLE 1. CODED EXPERIMENTAL RANGE AND LEVELS OF INDEPENDENT VARIABLES

Variable	Range and levels					
	Code	-1.68	-1	0	1	1.68
Reaction temperature (°C)	X_1	63.18	70	80	90	96.82
Catalyst weight (g)	X_2	0.30	1	2	3	3.68
Reaction time (min)	X_3	69.54	90	120	150	170.46

RESULTS AND DISCUSSION

Effect of Ratio of Zeolite to Sugar Cane

The effect of the weight ratio of zeolite to sugar cane over carbon zeolite catalyst yield and the weight ratio of zeolite to sulfonated carbon over catalyst acidity as well are shown in *Figure 1*.

Figure 1a shows that the weight ratio of zeolite-sugar cane (3:1) resulted in the highest zeolite-carbon yield of 67.78% compared to others, which indicated that the greater the amount of zeolite added, the greater the yield of zeolite-carbon produced. The yield also shows that the water and volatile materials have been evaporated in this process. *Figure 1b* shows that the weight ratio of zeolite-sulfonated carbon (3:1) resulted in the highest zeolite-carbon acidity of 10.80 mmol g^{-1} compared to others. The H$^+$ ion bound to the sulfonate group acts as the catalyst's active site. The catalyst acidity

tends to decrease until it finally increases again. The enormous acidity value indicates that the more polycyclic aromatic hydrocarbons formed, the more ortho polycyclic aromatic hydrocarbons could be attacked by electrophiles (-SO$_3$H).

Figure 2 shows the FTIR spectra of the zeolite-sulfonated carbon. From *Figure 2a*, FTIR spectra of carbon shows an absorption near 3417.00 cm^{-1}, which suggests the presence of hydroxyl vibrations. Strong absorption was also observed in the area of 1627.92 cm^{-1}, whereby corresponded to the existence of an aromatic ring; this indicated that the carbon only contained an aromatic ring and an OH group, without any functionalised sulfonate group in the sugar cane carbon. Subsequently, zeolite-sulfonated carbon of 1:3, 1:1 and 2:1 in *Figure 2* show that the zeolite-sulfonated carbon composite of each catalyst had a strong absorption of -SO$_3$H at 1064.71, 1064.70 and 1072.42 cm^{-1}, respectively (Hajamini *et al.*, 2016). Furthermore, the zeolite-sulfonated carbon of 1:3, 1:1 and 2:1 had width absorption bands of 3416.82, 3448.72 and 3417.86 cm^{-1}, respectively, associated with O-H vibrational ranges (Lathiya *et al.*, 2018). The aromatic ring at 1650-1450 cm^{-1} zeolite-sulfonated carbon was observed in the absorption peaks of 1627.92 cm^{-1} as well as 1635.64 cm^{-1}, respectively, in this way inherently demonstrated that the aromatic ring had functionalised by the sulfonated group. This sulfonate group acted as the active site of the zeolite-sulfonated carbon catalyst.

The catalyst's SEM analysis is shown in *Figure 3* with x5000 magnification. The surface morphology of the zeolite-sulfonated carbon catalyst (1:3) shows
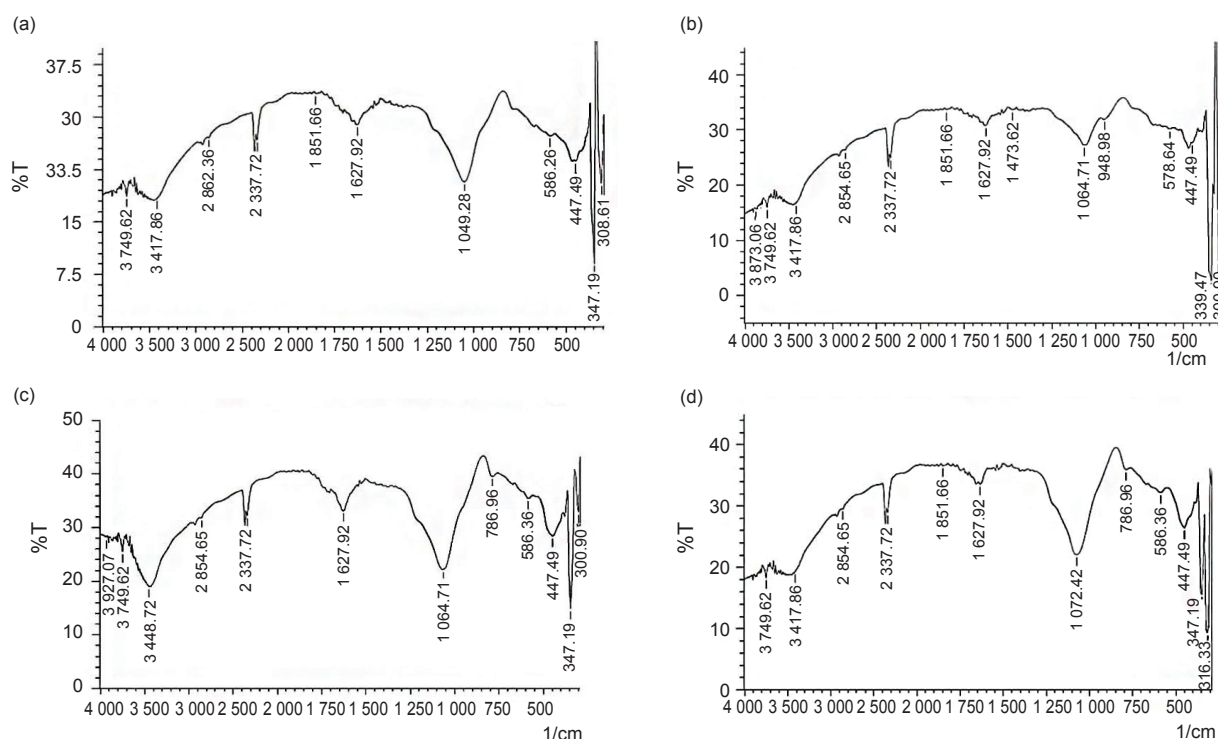

Figure 2. FTIR spectrum of (a) carbon, (b) 1:3, (c) 1:1, and (d) 2:1 zeolite-sulfonated carbon catalyst.
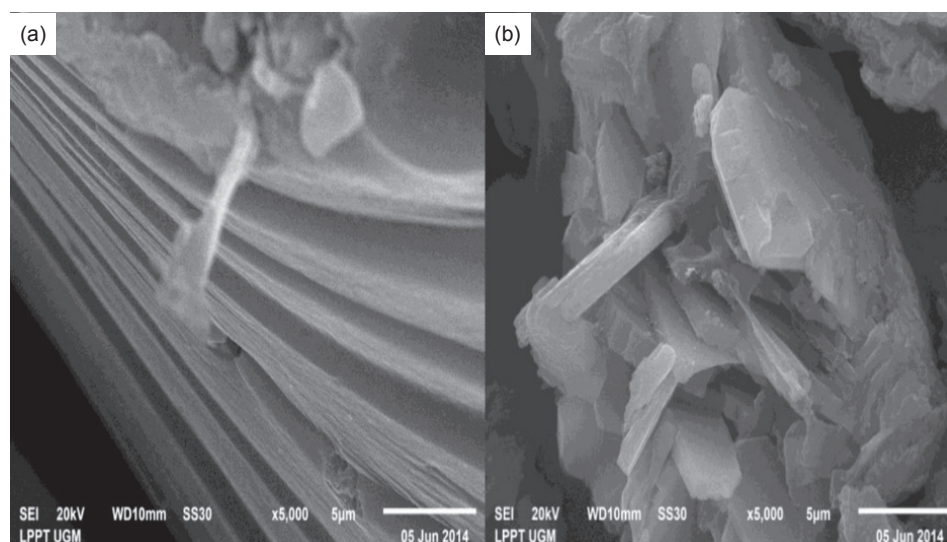
Figure 3. SEM analysis of (a) sulfonated carbon, and (b) zeolite-sulfonated carbon catalyst.

a surface with slightly rough characteristics, and thick and long fibrous granules, whereas, on the carbon sulfonate catalyst, the surface morphology was smooth, dense multi-layered. The zeolite-sulfonated carbon elemental composition was assessed using EDX. The EDX result shows that the zeolite-sulfonated carbon catalyst has elements of C with a mass of 36.47%, Si of 13.22% and S of 0.49%, whereas the sulfonated carbon catalyst has a mass of carbon elements of 61.94%, Si of 0.11% and S of 0.49%. The presence of element S as a sulfonate group attached to the zeolite-carbon indicated that there was a sulfonate group in the catalyst. Based on the results of the study, a zeolite-sulfonated carbon catalyst with the ratio of 1:3 (% w/w) was used for the esterification reaction because it has the greatest acidity value.

Fatty Acid in SPO

Analysis of fatty acids in SPO using GC shows that SPO contained palmitic acid at 60.21% as the highest fatty acid, accompanied by oleic acid at 17.44%. The FFA on SPO obtained an average value of 85.38%; this shows that SPO from PT Agro Indralaya Mandiri could be processed into esters because SPO had free fatty acids that could be reacted with alcohol.

Modelling Results and ANOVA

The reduced cubic model in coded form for the conversion of FFA (Y) was shown in Equation (2) as follow:

Conversion $(Y) = 089.67 + 0.1784X_1 + 6.35X_2 + 0.7135X_3 - 1.59X_1X_2 - 3.00X_1X_3 - 0.2187X_2X_3 + 2.44X_1^2 - 2.38X_2^2 - 2.38X_3^2 + 5.74X_1X_2X_3 - 4.03X_1^2X_2 + 0.6502X_1^2X_3 + 5.45X_1X_2^2$ (2)

The positive sign in Equation (2) shows a synergistic effect on the FFA conversion whereas the negative sign shows the opposite effect.

According to the statistical analysis, the greater F-value and the smaller *p*-value indicated that the coefficient which corresponded to the model was increasingly significant (Behera *et al.*, 2018). It shows that the F_{model} was 2887.10, whereas F_{table} = F(13; 16; 0.05) was 2.40. Since $F_{model} > F_{table}$, this designated that the model obtained was statistically significant. The *p*-value also shows that the variable model was significant. The model's importance could be strengthened by looking at the Lack of Fit. F_{model} for Lack of Fit was 1.46, whereas F_{table}= F(1; 16; 0.05) was 4.49. Since $F_{model} < F_{table}$, this implied that the Lack of Fit was insignificant, which indicated that the proposed model was suitable with experimental data and independent variables provided a sizeable effect on the response (Adepoju, 2020).

The signal/noise ratio was calculated with adequate precision, which consists of the predicted response derived from the model and the average prediction error. The ratio of adequacy precision obtained in this experiment was greater than 4; indicating a good adequacy precision ratio for experimental data (Đặng *et al.*, 2017). The sufficiency of the proposed model was a major role in checking the model analysis. The normal and studentised residual probability were analysed for the FFA conversion are shown in supplementary data. It can be seen that all response values, random scatter plots, and observed variance were constant, and this indicated that there was no need to transform the response variable (Helmi *et al.*, 2021). The calculated absolute error did not exceed 1.00% error, is in the range between 0.05%-0.22%; this indicated that the model met the criteria to be

within the 95.00% confidence interval (Samuel *et al.*, 2020) and proposed an adequate model (Hasanudin *et al.*, 2022a).

The statistical parameters obtained from ANOVA show that the R^2 and adjusted R^2 (R_{adj}) values were obtained at 0.9999 and 0.9996, respectively. The value of R^2 described the extent to which the model could estimate the experimental data points and R_{adj} calculated the sum of variation in the mean value described by the proposed model (Adepoju, 2020). The predicted R^2 for Equation (2) was 0.9924 and precisely to the R^2 value, this revealed that the experimental results for the FFA conversion were in accordance with the model prediction value. The model's standard deviation was 0.1783; indicating a good model that matched the predicted with the actual value for the response (Pascoal *et al.*, 2020).

The Combination Influence of Reaction Temperature, Time and Catalyst Weight on the FFA Conversion

The effect of the factor on the FFA conversion and the three-dimensional (3D) response surface were plotted. The experimental outcome of FFA conversion is as *Table 2*.

TABLE 2. THE EXPERIMENTAL DATA OF FFACONVERSION

No.	Temperature (°C)	Reaction time (min)	Catalyst weight (g)	Y (%)
1	70.00	90.00	1.00	70.50
2	90.00	90.00	1.00	79.83
3	70.00	90.00	3.00	89.46
4	90.00	90.00	3.00	71.03
5	70.00	150.00	1.00	90.37
6	90.00	150.00	1.00	66.29
7	70.00	150.00	3.00	87.05
8	90.00	150.00	3.00	78.02
9	63.18	120.00	2.00	82.54
10	96.82	120.00	2.00	83.14
11	80.00	120.00	0.30	72.31
12	80.00	120.00	3.68	93.68
13	80.00	69.54	2.00	72.31
14	80.00	170.46	2.00	74.71
15	80.00	120.00	2.00	89.76
16	80.00	120.00	2.00	89.75
17	80.00	120.00	2.00	89.47

Figure 4 shows the combined influence of catalyst weight (X_2) and reaction time (X_3) on the conversion of FFA at constant temperature (80°C) and the effect of the combination of reaction temperature (X_1) and time (X_3) on the conversion of FFA at constant catalyst weight (2 g), respectively.

Figure 4a shows that the maximum FFA conversion was achieved at a catalyst weight of 2.00-3.68 g and a reaction time of 100-140 min. This statement was validated with the optimal condition of catalyst weight of 3.68 g along with a reaction time of 120 min resulting in an experimental conversion of 93.68%, and in this condition, it gave an FFA content of 5.39%. This indicated that there was a decrease in FFA on the ester product. The more catalyst used, the more Lewis and Brønsted acid active sites. This acid site lowers the activation energy, which speeds up the esterification reaction rate resulting in a high conversion (Anguebes-Franseschi *et al.*, 2018). Contrastingly, if the reaction time was too short, less than 100 min, the collision between the reactants and the catalyst will be less effective. As a result, conversion was relatively low (Levenspiel, 1964), and if the reaction time was too long, more than 140 min, the resulting conversion will relatively decrease. The reduction in the conversion yield over the longer reaction time was likely due to the formation of by-products or deactivation of the active sites of the catalyst (Chellappan *et al.*, 2019). This condition was consistently reported by Jenie *et al.* (2020) for oleic acid esterification using sulfonated magnetic biochar catalyst. Hidayat and Sutrisno (2017) reported that the ZrO_2/SO_4^{-2} combined rice husk catalyst provided up to 83.10% FFA conversion derived from SPO using 10%wt catalyst and 60°C, whereas Abdullah *et al.* (2017) used alum as a catalyst and generated up to 90.00% FFA. Furthermore, Hayyan *et al.* (2010) showed that the 0.75%wt of toluene-4-sulfonic monohydrate acid (PTSA) catalyst exhibited FFA conversion up to 80.00%.

Figure 4b shows that the maximum FFA conversion was attained at a reaction temperature of 70°C-90°C and 100-140 min reaction. Generally, an increase in reaction temperature esterification reaction will give higher conversion due to an increase in reaction rate. As the temperature increases, the viscosity of the solution diminishes and makes mixing better (Ong *et al.*, 2014). However, a reaction temperature that was too high will have a negative influence on the conversion, this was probably due to the reduction of methanol from the liquid phase to the gas phase, thereby minimising the esterification reaction process and making the conversion relatively low (Qu *et al.*, 2020). In addition, too low a reaction temperature did not significantly increase the conversion rate. The reaction at low temperature will take more time to complete than at high temperature (Marwaha *et al.*, 2019). Ibrahim
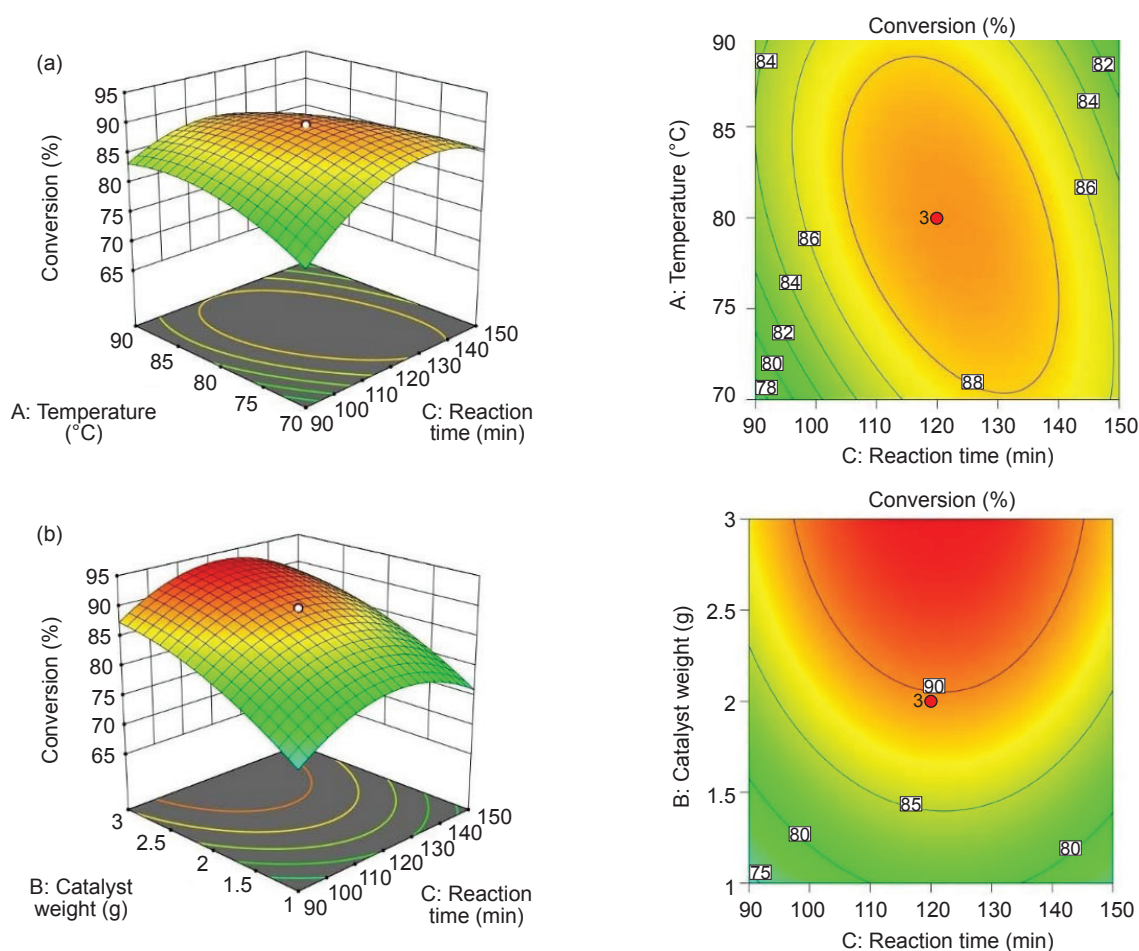
Figure 4. (a) Effect of combination of catalyst weight and reaction time, (b) effect of the combination of temperature and reaction time on FFA conversion.

et al. (2020) used sulfonated carbon from corncob waste for FFA esterification from PFAD and showed that the increment of reaction temperature from 65°C to 70°C promotes FFA conversion up to 92.00%. Nevertheless, if the reaction temperature was too high, it caused a decrement in FFA conversion up to 90.00%. The study also reported that 2 hr of esterification exhibited a high conversion of 92.00%. Hayyan *et al.* (2010) showed that a high conversion of FFA derived from SPO was achieved up to 90.93% when a temperature at 60°C and 60 min reaction using PTSA catalyst.

Optimisation and Validation

The FFA conversion optimisation was executed by the numerical method (Pascoal *et al.*, 2020) and the maximum option was selected as the main factor *i.e.*, catalyst weight, reaction temperature and reaction time. According to the optimisation process, variables in optimum conditions for conversion were accomplished at a reaction temperature of 78.98°C, a reaction time of 119.97 min, catalyst weight of 2.97 g and an FFA conversion of 94.19%. Additional experiments were performed and showed that the experimental result was close to the predicted response by the model. It could be concluded that the mathematical model obtained in the RSM-CCD can accurately predict the conversion to obtain optimum conditions.

Esterification Products Analysis using ¹³C-NMR

The analysis of SPO and products at optimum conditions using ¹³C-NMR spectroscopy is shown in *Figure 5*.

The results of the identification of esterification products showed that there was a typical C=O signal of ester at a chemical shift around 176.00 ppm, and at 180.31 ppm, there was no signal indicating that esterification occurred which the carboxyl group as FFA turned into ester products (Tariq *et al.*, 2011). The ester products are also identified by the presence of the C-methoxy signal, which is a representative carbon in the ester with a chemical shift of 51.44 ppm (Munir *et al.*, 2021). Apart from C=O ester and methoxy, the spectrum shows a high peak at the chemical shift of 49.74 ppm, indicating there was still methanol leftover from the esterification reaction.

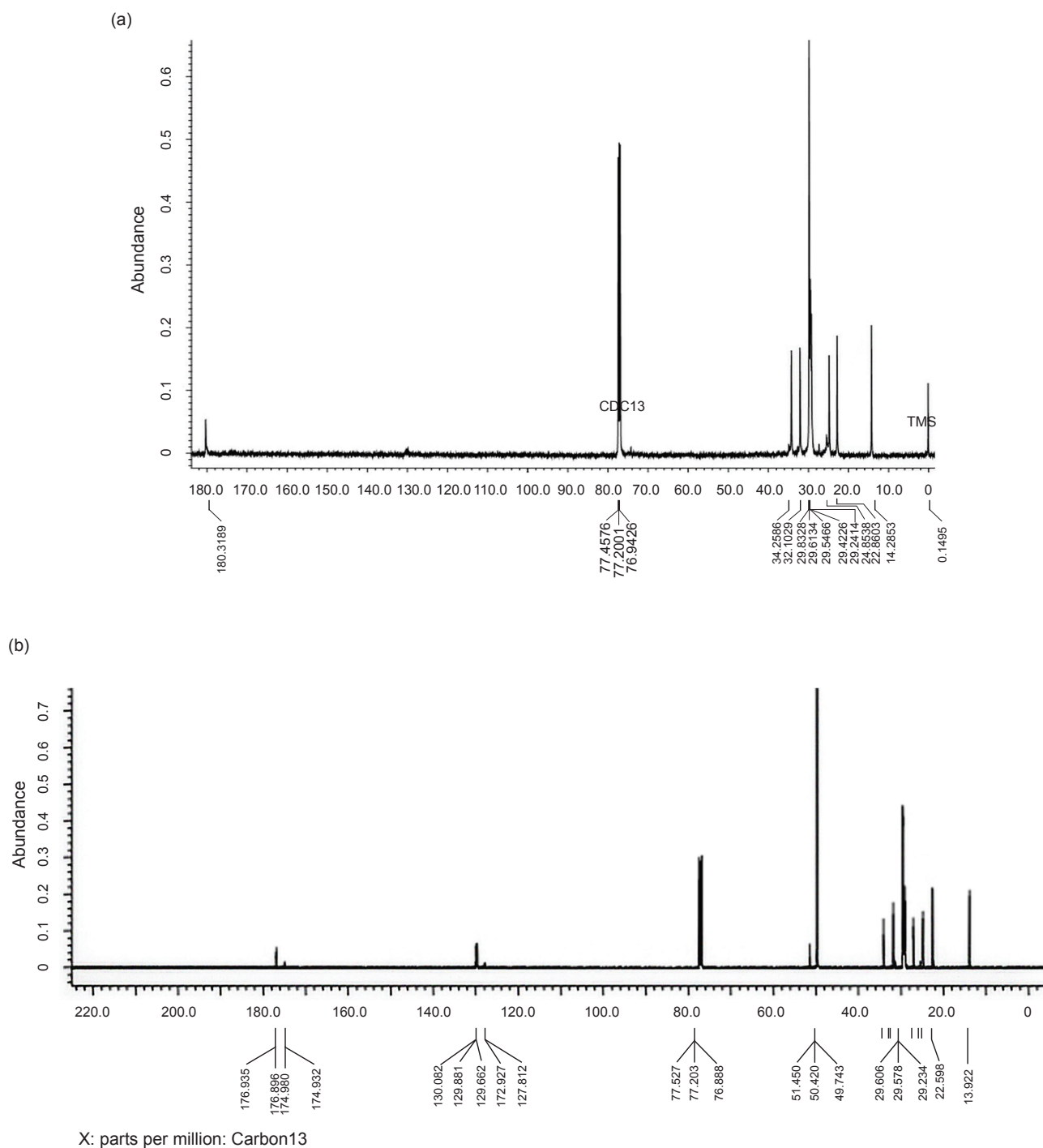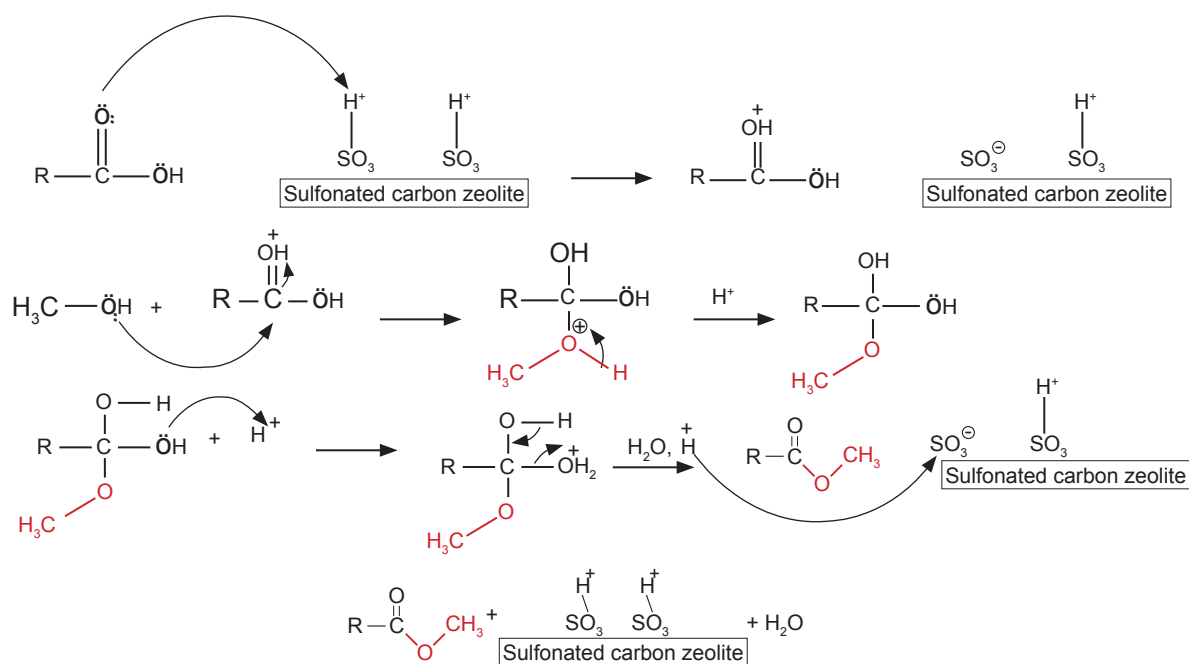The proposed mechanism of esterification reaction using zeolite-sulfonated carbon is

(a)

(b)

X: parts per million: Carbon13

Figure 5. The ^{13}C-NMR spectrum of (a) SPO and (b) esterification product.

shown in *Figure 6* (Hasanudin *et al.*, 2022b). The formation of esters using a zeolite-sulfonated carbon composite catalyst went through a two-step process; that was the attack of unprotected phi (π) electrons in the ethanol double bond, which would attract electrophiles (H^+) on the catalyst; hence a carbocation was produced at C_1 ethanol compounds. Subsequently, the carbocation was attacked by the nucleophile (CH_3COOH^-), resulting in an ester product.

Catalyst Reusability

The study of catalyst reusability was conducted on the optimum condition employed by RSM-CCD using zeolite-sulfonated carbon from sugar cane catalyst. The catalyst was washed with methanol and then reused after drying. *Figure 7* shows the reusability accession of FFA conversion derived from SPO up to four times reused.

Source: Hasanudin *et al.* (2022b).

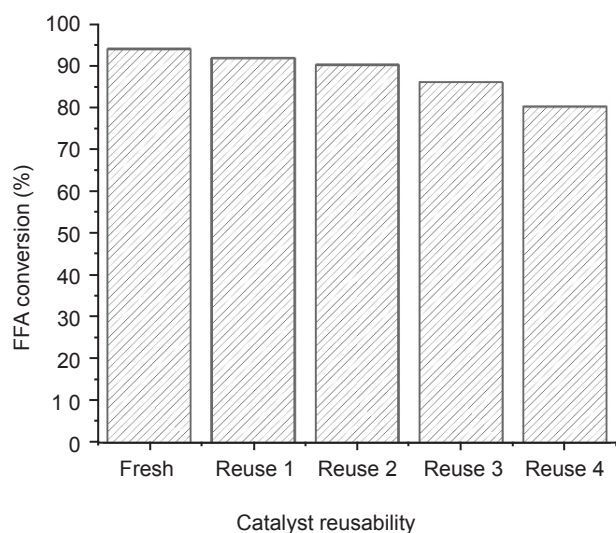*Figure 6. Proposed mechanism of esterification reaction using zeolite-sulfonated carbon.*

Figure 7. Reusability of catalyst.

It can be noticed that the FFA conversion decreased with the incrementing catalyst reuse cycle. Previous studies also reported a similar finding using various sulfonated carbon-based catalysts (Balan *et al.*, 2021; Ballotin *et al.*, 2020; Peng *et al.*, 2010). *Figure 7* appears that FFA conversion decreased from 94.20% to 92.03%, indicating that the catalyst performance decreased by 7.51%. The second and third cycles generated 90.44% and 86.23% conversions, with a drop in catalyst performance of 9.01% and 12.97%, respectively.

Furthermore, the reaction with the fourth cycle was only able to produce a conversion of 80.42%, with a lower catalyst performance decreased by 18.44%. The decrease in catalytic activity might be due to the leaching of the $-SO_3H$ active (Tang and Niu, 2019). Methanol could dissolve fatty acid interaction with the catalyst. However, methanol washing causes a decrease in catalytic performance by forming methyl sulfonate from the reaction of methanol with sulfonate groups. Thus, the active functional groups of the catalyst are reduced and lead to lower catalytic activity (Dawodu *et al.*, 2014).

In this research, the zeolite-sulfonated carbon derived from sugar cane catalyst composite has been employed for the esterification of FFA from SPO and optimised by RSM-CCD. The study suggested that the catalyst could be potentially upgraded up to mass-produce for the practical application as an FFA esterification catalyst, as indicated by relatively good catalyst reusability and high FFA conversion. The high FFA content of SPO also provided a primary option as a FAME feedstock as well as leading to the valorisation of SPO waste into value-added oil. However, since this study conducted reaction in the batch system, it is necessary to conduct future studies using the continuous system. This system would provide better economic feasibility and improve the reaction process. Further study regarding the kinetic parameters also needed to be evaluated to understand the esterification process comprehensively.

CONCLUSION

The RSM-CCD was applied to optimise the conversion of free fatty acids into biodiesel from SPO using a zeolite-sulfonated carbon composite catalyst. SPO had a high content of FFA which had potential as a feedstock for biodiesel production. The zeolite-sulfonated carbon composite catalyst (1:3) (% w/w) was chosen as the best catalyst as it revealed the highest acidity compared to other catalyst weight ratios. FTIR analysis of zeolite-sulfonated carbon (1:3) catalyst showed the presence of sulfonate group absorption which was confirmed by SEM-EDX analysis. The ^{13}C-NMR analysis of the products showed a chemical shift of 176 ppm for C=O ester, 51.45 ppm and 50.42 ppm for C-methoxy. The optimum condition for the conversion was acquired at a reaction temperature of 78.98°C, a reaction time of 119.97 min, catalyst weight of 2.97 g, with an FFA conversion of 94.19%. The reduced cubic mathematical model was successful in predicting the response with a minimal percentage of error. The catalyst reusability analysis demonstrated that the catalyst had a minor decline in catalyst performance and could generate up to 80.00% FFA conversion after the fourth cycle.

REFERENCES

Abdullah; Sianipar, R R N; Ariyani, D and Nata, I F (2017). Conversion of palm oil sludge to biodiesel using alum and KOH as catalysts. *Sustain. Environ. Res.*, *27(6)*: 291-295. DOI: 10.1016/j.serj.2017. 07.002.

Adepoju, T F (2020). Optimization processes of biodiesel production from pig and neem (*Azadirachta Indica* A. Juss) seeds blend oil using alternative catalysts from waste biomass. *Ind. Crops Prod.*, *149*: 112334. DOI: 10.1016/j. indcrop.2020.112334.

Anguebes-Franseschi, F; Abatal, M; Bassam, A; Soberanis, M A E; Tzuc, O M; Bucio-Galindo, L; Quiroz, A V C; Ucan, C A A and Ramirez-Elias, M A (2018). Esterification optimization of crude African palm olein using response surface methodology and heterogeneous acid catalysis. *Energies*, *11(1)*: 157. DOI: 10.1016/j.wasman.2019.09.030.

Arumugamurthy, S S; Sivanandi, P; Pandian, S; Choksi, H and Subramanian, D (2019). Conversion of a low value industrial waste into biodiesel using a catalyst derived from brewery waste: An activation and deactivation kinetic study. *Waste Manag.*, *100*: 318-326. DOI: 10.1016/j.wasman.2019. 09.030.

Aslan, V and Eryilmaz, T (2020). Polynomial regression method for optimization of biodiesel production from black mustard (*Brassica nigra* L.) seed oil using methanol, ethanol, NaOH, and KOH. *Energy*, *209*: 118386. DOI: 10.1016/j. energy.2020.118386.

Balan, W S; Janaun, J; Chung, C H; Semilin, V; Zhu, Z; Haywood, S K; Touhami, D; Chong, K P; Yaser, A Z; Lee, P C and Zein, S H (2021). Esterification of residual palm oil using solid acid catalyst derived from rice husk. *J. Hazard. Mater.*, *404*: 124092. DOI: 10.1016/j.jhazmat.2020.124092.

Ballotin, F C; Da Silva, M J; Lago, R M and Teixeira, A P D C (2020). Solid acid catalysts based on sulfonated carbon nanostructures embedded in an amorphous matrix produced from bio-oil: Esterification of oleic acid with methanol. *J. Environ. Chem. Eng.*, *8(2)*: 103674. DOI: 10.1016/j.jece.2020.103674.

Behera, S K; Meena, H; Chakraborty, S and Meikap, B C (2018). Application of response surface methodology (RSM) for optimization of leaching parameters for ash reduction from low-grade coal. *Int. J. Min. Sci. Technol.*, *28(4)*: 621-629. DOI: 10.1016/j. ijmst.2018.04.014.

Chellappan, S; Aparna, K; Chingakham, C; Sajith, V and Nair, V (2019). Microwave assisted biodiesel production using a novel Brønsted acid catalyst based on nanomagnetic biocomposite. *Fuel*, *246*: 268-276. DOI: 10.1016/j.fuel.2019.02.104.

Đặng, T H; Chen, B H and Lee, D J (2017). Optimization of biodiesel production from transesterification of triolein using zeolite LTA catalysts synthesized from kaolin clay. *J. Taiwan Inst. Chem. Eng.*, *79*: 14-22. DOI: 10.1016/j.jtice.2017.03.009.

Dawodu, F A; Ayodele, O; Xin, J; Zhang, S and Yan, D (2014). Effective conversion of non-edible oil with high free fatty acid into biodiesel by sulphonated carbon catalyst. *Appl. Energy*, *114*: 819-826. DOI: 10.1016/j.apenergy.2013.10.004.

Farabi, M S A; Ibrahim, M L; Rashid, U and Taufiq-Yap, Y H (2019). Esterification of palm fatty acid

distillate using sulfonated carbon-based catalyst derived from palm kernel shell and bamboo. *Energy Convers. Manag.*, *181*: 562-570. DOI: 10.1016/j.enconman.2018.12.033.

Fonseca, J M; Spessato, L; Cazetta, A L; Bedin, K C; Melo, S A R; Souza, F L and Almeida, V C (2020). Optimization of sulfonation process for the development of carbon-based catalyst from crambe meal via response surface methodology. *Energy Convers. Manag.*, *217*: 112975. DOI: 10.1016/j.enconman.2020.112975.

Garritano, A N; Faber, M de O; De Sà, L R V and Ferreira-Leitão, V S (2018). Palm oil mill effluent (POME) as raw material for biohydrogen and methane production via dark fermentation. *Renew. Sustain. Energy Rev.*, *92*: 676-684. DOI: 10.1016/j.rser.2018.04.031.

Goh, C L; Sethupathi, S; Bashir, M J and Ahmed, W (2019). Adsorptive behaviour of palm oil mill sludge biochar pyrolyzed at low temperature for copper and cadmium removal. *J. Environ. Manage.*, *237*: 281-288. DOI: 10.1016/j.jenvman.2018.12.103.

Guo, Z; Wu, J; Zhang, Y; Cao, K; Feng, Y; Liu, J and JIan, L (2020). Briquetting optimization method for the lignite powder using response surface analysis. *Fuel*, *267*: 117260. DOI: 10.1016/j.fuel.2020.117260.

Hajamini, Z; Sobati, M A; Shahhosseini, S and Ghobadian, B (2016). Waste fish oil (WFO) esterification catalyzed by sulfonated activated carbon under ultrasound irradiation. *Appl. Therm. Eng.*, *94*: 1-10. DOI: 10.1016/j.applthermaleng.2015.10.101.

Hasanudin, H; Asri, W R; Said, M; Hidayati, P T; Purwaningrum, W; Novia, N and Wijaya, K (2022a). Hydrocracking optimization of palm oil to bio-gasoline and bio-aviation fuels using molybdenum nitride-bentonite catalyst. *RSC Adv.*, *12(26)*: 16431-16443.

Hasanudin, H; Putri, Q U; Agustina, T E and Hadiah, F (2022b). Esterification of free fatty acid in palm oil mill effluent using sulfated carbon-zeolite composite catalyst. *Pertanika J. Sci. Technol.*, *30(1)*: 377-395. DOI: 10.47836/pjst.30.1.21.

Hayyan, A; Alam, M Z; Mirghani, M E S; Kabbashi, N A; Hakimi, N I N M; Siran, Y M and Tahiruddin, S (2011). Reduction of high content of free fatty acid in sludge palm oil via acid catalyst for biodiesel production. *Fuel Process. Technol.*, *92(5)*: 920-924. DOI: 10.1016/j.fuproc.2010.12.011.

Hayyan, A; Alam, M Z; Mirghani, M E S; Kabbashi, N A; Hakimi, N I N M; Siran, Y M and Tahiruddin, S (2010). Sludge palm oil as a renewable raw material for biodiesel production by two-step processes. *Bioresour. Technol.*, *101(20)*: 7804-7811. DOI: 10.1016/j.biortech.2010.05.045.

Helmi, M; Tahvildari, K; Hemmati, A and Aberoomand, P (2021). Phosphomolybdic acid/graphene oxide as novel green catalyst using for biodiesel production from waste cooking oil via electrolysis method: Optimization using with response surface methodology (RSM). *Fuel*, *287*: 119528. DOI: 10.1016/j.fuel.2020.119528.

Hidayat, A and Sutrisno, B (2017). Esterification free fatty acid in sludge palm oil using ZrO_2/SO_4^{2-}-Rice husk ash catalyst. *AIP Conf. Proc.*, *1840(1)*: 050001. DOI: 10.1063/1.4982275.

Ibrahim, S F; Asikin-Mijan, N; Ibrahim, M L; Abdulkareem-Alsultan, G; Izham, S M and Taufiq-Yap, Y H (2020). Sulfonated functionalization of carbon derived corncob residue via hydrothermal synthesis route for esterification of palm fatty acid distillate. *Energy Convers. Manag.*, *210*: 112698. DOI: 10.1016/j.enconman.2020.112698.

Jenie, S N A; Kristiani, A; Sudiyarmanto; Khaerudini, D S and Takeishi, K (2020). Sulfonated magnetic nanobiochar as heterogeneous acid catalyst for esterification reaction. *J. Environ. Chem. Eng.*, *8(4)*: 103912. DOI: 10.1016/j.jece.2020.103912.

Junior, W A G P; Takeno, M L; Nobre, F X; Barros, S de S; Sá, I S C; Silva, E P; Manzato, L; Iglauer, S and de Freitas, F A (2020). Application of water treatment sludge as a low-cost and eco-friendly catalyst in the biodiesel production via fatty acids esterification: Process optimization. *Energy*, *213*: 118824. DOI: 10.1016/j.energy.2020.118824.

Kenawy, I M M; Eldefrawy, M M; Eltabey, R M and Zaki, E G (2019). Melamine grafted chitosan-montmorillonite nanocomposite for ferric ions adsorption: Central composite design optimization study. *J. Clean. Prod.*, *241*: 118189. DOI: 10.1016/j.jclepro.2019.118189.

Ketzer, F; Celante, D and de Castilhos, F (2020). Catalytic performance and ultrasonic-assisted impregnation effects on WO3/USY zeolites in esterification of oleic acid with methyl acetate. *Microporous Mesoporous Mater.*, *291*: 109704. DOI: 10.1016/j.micromeso.2019.109704.

Lathiya, D R; Bhatt, D V and Maheria, K C (2018). Synthesis of sulfonated carbon catalyst from waste orange peel for cost effective biodiesel production.

Bioresour. Technol. Reports, 2: 69-76. DOI: 10.1016/j. biteb.2018.04.007.

Lawan, I; Garba, Z N; Zhou, W; Zhang, M and Yuan, Z (2020). Synergies between the microwave reactor and CaO/Zeolite catalyst in waste lard biodiesel production. *Renew. Energy*, 145: 2550-2560. DOI: 10.1016/j.renene.2019.08.008.

Levenspiel, O (1964). *Chemical Reaction Engineering*. 3rd edition. Wiley. New York. 671 pp.

Liu, X; Zhu, F; Zhang, R; Zhao, L and Qi, J (2021). Recent progress on biodiesel production from municipal sewage sludge. *Renew. Sustain. Energy Rev.*, 135: 110260. DOI: 10.1016/j.rser.2020. 110260.

Manojkumar, N; Muthukumaran, C and Sharmila, G A (2020). Comprehensive review on the application of response surface methodology for optimization of biodiesel production using different oil sources. *J. King Saud Univ. - Eng. Sci.*, 34(3): 198-208. DOI: 10.1016/j.jksues.2020.09.012.

Marwaha, A; Rosha, P; Mohapatra, S K; Mahla, S K and Dhir, A (2019). Biodiesel production from *Terminalia bellerica* using eggshell-based green catalyst: An optimization study with response surface methodology. *Energy Reports*, 5: 1580-1588. DOI: 10.1016/j.egyr.2019.10.022.

Muanruksa, P and Kaewkannetra, P (2020). Combination of fatty acids extraction and enzymatic esterification for biodiesel production using sludge palm oil as a low-cost substrate. *Renew. Energy*, 146: 901-906. DOI: 10.1016/j.renene.2019.07.027.

Munir, M; Ahmad, M; Mubashir, M; Asif, S; Waseem, A; Mukhtar, A; Saqib, S; Munawaroh, H S H; Lam, M K; Khoo, K S; Bokhari, A and Show, P L (2021). A practical approach for synthesis of biodiesel via non-edible seeds oils using trimetallic based montmorillonite nano-catalyst. *Bioresour. Technol.*, 328: 124859. DOI: 10.1016/j.biortech.2021.124859.

Nasution, M A; Wibawa, D S; Ahamed, T and Noguchic, R (2018a). Comparative environmental impact evaluation of palm oil mill effluent treatment using a life cycle assessment approach: A case study based on composting and a combination for biogas technologies in North Sumatera of Indonesia. *J. Clean. Prod.*, 184: 1028-1040. DOI: 10.1016/j. jclepro.2018.02.299.

Nasution, M A; Wibawa, D S; Ahamed, T and Noguchi, R (2018b). Selection of palm oil mill effluen treatment for biogas generation or compost production using an analytic hierarchy process.

J. Mater. Cycles Waste Manag., 20(2): 787-799. DOI: 10.1007/s10163-017-0638-9.

Ngaosuwan, K; Goodwin, J G and Prasertdham, P (2016). A green sulfonated carbon-based catalyst derived from coffee residue for esterification. *Renew. Energy*, 86: 262-269. DOI: 10.1016/j. renene.2015.08.010.

Ong, H C; Masjuki, H H; Mahlia, T M I; Silitonga, A S; Chong, W T and Leong, K Y (2014). Optimization of biodiesel production and engine performance from high free fatty acid *Calophyllum inophyllum* oil in CI diesel engine. *Energy Convers. Manag.*, 81: 30-40. DOI: 10.1016/j.enconman.2014.01.065.

Pascoal, C V P; Oliveira, A L L; Figueiredo, D D and Assunção, J C C (2020). Optimization and kinetic study of ultrasonic-mediated *in situ* transesterification for biodiesel production from the almonds of *Syagrus cearensis*. *Renew. Energy*, 147: 1815-1824. DOI: 10.1016/j.renene.2019.09.122.

Peng, L; Philippaerts, A; Ke, X; Van Noyen, J; De Clippel, F; Van Tendeloo, G; Jacobs, P A and Sels, B F (2010). Preparation of sulfonated ordered mesoporous carbon and its use for the esterification of fatty acids. *Catal. Today*, 150(1-2): 140-146. DOI: /10.1016/j.cattod.2009.07.066.

Qu, T; Niu, S; Gong, Z; Han, K; Wang, Y and Lu, C (2020). Wollastonite decorated with calcium oxide as heterogeneous transesterification catalyst for biodiesel production: Optimized by response surface methodology. *Renew. Energy*, 159: 873-884. DOI: 10.1016/j.renene.2020.06.009.

Quah, R V; Tan, Y H; Mubarak, N M; Khalid, M; Abdullah, E C and Nolasco-Hipolito, C (2019). An overview of biodiesel production using recyclable biomass and non-biomass derived magnetic catalysts. *J. Environ. Chem. Eng.*, 7(4): 103219. DOI: 10.1016/j.jece.2019.103219.

Rahman, N; Giller, K E; de Neergaard, A; Magid, J; van de Ven, G and Bruun, T B (2021). The effects of management practices on soil organic carbon stocks of oil palm plantations in Sumatra, Indonesia. *J. Environ. Manage.*, 278: 111446. DOI: 10.1016/j. jenvman.2020.111446.

Samuel, O D; Okwu, M O; Oyejide, O J; Taghinezhad, E; Afzal, A and Kaveh, M (2020). Optimizing biodiesel production from abundant waste oils through empirical method and grey wolf optimizer. *Fuel*, 281: 118701. DOI: 10.1016/j.fuel.2020.118701.

dos Santos, L K; Hatanaka, R R; de Oliveira, J E and Flumignan, D L (2019). Production of biodiesel

from crude palm oil by a sequential hydrolysis/esterification process using subcritical water. *Renew. Energy*, *130*: 633-640. DOI: 10.1016/j.renene.2018.06.102.

Sun, K; Lu, J; Ma, L; Han, Y; Fu, Z and Ding, J (2015). A comparative study on the catalytic performance of different types of zeolites for biodiesel production. *Fuel*, *158*: 848-854. DOI: 10.1016/j.fuel.2015.06.048.

Tang, P L; Hong, W L; Yue, C S and Harun, S (2020). Palm oil mill effluent as the pretreatment solvent of oil palm empty fruit bunch fiber for fermentable sugars production. *Bioresour. Technol.*, *314*: 123723. DOI: 10.1016/j.biortech.2020.123723.

Tang, Z E; Lim, S; Pang, Y L; Ong, H C and Lee, K T (2018). Synthesis of biomass as heterogeneous catalyst for application in biodiesel production: State of the art and fundamental review. *Renew. Sustain. Energy Rev.*, *92*: 235-253. DOI: 10.1016/j.rser.2018.04.056.

Tang, X and Niu, S (2019). Preparation of carbon-based solid acid with large surface area to catalyze esterification for biodiesel production. *J. Ind. Eng. Chem.*, *69*: 187-195. DOI: 10.1016/j.jiec.2018.09.016.

Tao, M L; Guan, H Y; Wang, X H; Liu, Y C and Louh, R F (2015). Fabrication of sulfonated carbon catalyst from biomass waste and its use for glycerol esterification. *Fuel Process. Technol.*, *138*: 355-360. DOI: 10.1016/j.fuproc.2015.06.021.

Tariq, M; Ali, S; Ahmad, F; Ahmad, M; Zafar, M; Khalid, N and Khan, M A (2011). Identification, FT-IR, NMR (1H and 13C) and GC/MS studies of fatty acid methyl esters in biodiesel from rocket seed oil. *Fuel Process. Technol.*, *92(3)*: 336-341. DOI: 10.1016/j.fuproc.2010.09.025.

Zhang, B; Gao, M; Geng, J; Cheng, Y; Wang, X; Wu, C; Wang, Q; Liu, S and Cheung, S M (2021). Catalytic performance and deactivation mechanism of a one-step sulfonated carbon-based solid-acid catalyst in an esterification reaction. *Renew. Energy*, *164*: 824-832. DOI: 10.1016/j.renene.2020.09.076.